Title

Oestrogen engages brain MC4R signalling to drive physical activity in female mice

Journal

Nature, 599(7883)

ISSN

0028-0836

Authors

Krause, William C

Rodriguez, Ruben

Gegenhuber, Bruno

et al.

Publication Date

2021-11-04

DOI

10.1038/s41586-021-04010-3

Peer reviewed

HHS Public Access

Author manuscript

Nature. Author manuscript; available in PMC 2022 May 17.

Published in final edited form as:

Nature. 2021 November ; 599(7883): 131–135. doi:10.1038/s41586-021-04010-3.

Estrogen Drives Brain Melanocortin to Increase Physical Activity in Females

William C. Krause[1], **Ruben Rodriguez**[1], **Bruno Gegenhuber**[2,7], **Navneet Matharu**[3], **Andreas N. Rodriguez**[1], **Adriana M. Padilla-Roger**[4], **Kenichi Toma**[5], **Candice B. Herber**[1], **Stephanie M. Correa**[1,6], **Xin Duan**[5], **Nadav Ahituv**[3], **Jessica Tollkuhn**[7], **Holly A. Ingraham**[1]

[1]Department of Cellular and Molecular Pharmacology School of Medicine, University of California, San Francisco, CA 94143.

[2]Cold Spring Harbor Laboratory School of Biological Sciences, Cold Spring Harbor, NY 11724.

[3]Department of Bioengineering and Therapeutic Sciences and Institute for Human Genetics, University of California, San Francisco, CA 94143.

[4]Graduate Program in Neuroscience, UCSF.

[5]Departments of Ophthalmology and Physiology, University of California San Francisco, San Francisco, CA, 94143

[6]Present Address: Department of Integrative Biology and Physiology, University of California Los Angeles, Los Angeles, California 90095, USA.

[7]Cold Spring Harbor Laboratory, Cold Spring Harbor, NY 11724.

Abstract

Estrogen depletion in rodents and humans leads to inactivity, fat accumulation, and diabetes[1,2], underscoring the conserved metabolic benefits of estrogen that inevitably decline with aging. In rodents, the preovulatory surge in 17β-estradiol (E2) temporarily increases energy expenditure to coordinate increased physical activity with peak sexual receptivity. Here we uncover a subset of estrogen-sensitive neurons in the ventrolateral ventromedial hypothalamic nucleus (VMHvl)[3–7] that projects to arousal centers in the hippocampus and hindbrain and enables estrogen to rebalance energy allocation in females. Surges in E2 increase melanocortin-4 receptor (MC4R) signaling in these VMHvl neurons by directly recruiting estrogen receptor alpha (ERα) to the *Mc4r* gene. Sedentary behavior and obesity in estrogen-depleted females are reversed following chemogenetic stimulation of $VMHvl^{ERα/MC4R}$ neurons. Similarly, long-term elevation in physical activity is observed following CRISPR-mediated activation of this node. These data extend the impact of MC4R signaling – the most common cause of monogenic human obesity[8] – beyond the regulation of food intake and rationalize reported sex differences in melanocortin signaling, including greater disease severity of MC4R insufficiency in women[9]. This hormone-dependent node illuminates the power of estrogen during the reproductive cycle in motivating behavior and maintaining an active lifestyle, which are often diminished in postmenopausal women.

Co-corresponding Authors: holly.ingraham@ucsf.edu and tollkuhn@cshl.edu.

Keywords

Physical Activity; ERα; Mc4R; Estrogen; Menopause; Hormone Dependent Neurocircuits; Ventromedial Hypothalamus; CRISPRa

Estrogen Signaling In VMHvl Promotes Activity

To establish that females rely on VMHvl ERα signaling to maximize their spontaneous physical activity, we ablated ERα in the VMHvl or arcuate nucleus (ARC) of adult *Esr1*$^{fl/fl}$ female mice using stereotaxic delivery of AAV-Cre-GFP (VMHvl^{ERαKO}, ARC^{ERαKO}). Control female littermates received similarly targeted AAV-GFP (VMHvl^{Control} or ARC^{Control}). Reduced ambulatory activity was observed in VMHvl^{ERαKO} females during the dark (active) cycle that corresponded with a modest increase in body weight, a reduction of *Ucp1* in interscapular brown adipose tissue (iBAT), and unchanged food intake (Fig. 1a and Extended Data 1a-e). While we showed previously that ARC^{ERαKO} females exhibit a surprisingly high bone mass phenotype[4], no changes in activity, body weights, or food intake were noted in this cohort (Fig. 1a and Extended Data 1b). Normal food consumption, particularly in ARC^{ERαKO} females, suggests that estrogen's anorexigenic effects are mediated by extra-ARC sites[10] or masked by mouse strains/institutional housing conditions used here. When considered together with other ERα knockout mouse models, our data demonstrate a requirement for ERα in the VMHvl to maximize physical activity levels in adult female mice.

Hormone responsiveness of VMHvl^{ERα} neurons was visualized across the estrous cycle by monitoring phosphorylated ribosomal protein S6 (pS6) during estrus (low E2) and proestrus (high E2). VMHvl pS6 signals rise substantially during proestrus or following an estradiol benzoate (EB) injection into ovariectomized (OVX) females (Fig. 1b, c and Extended Data 2a), but were negligible during estrus, in females lacking ERα, or in intact, untreated males (Extended Data 2b,c), underscoring a complete dependence of this pS6 response on both estrogen and ERα. Estrogen induction of pS6 in VMHvl^{ERα} neurons occurs via a classical genomic mechanism that begins slowly starting 2 hrs post-treatment. By contrast, no hormone-dependent pS6 induction was detected in adjacent ARC^{ERα} neurons (Fig. 1c and Extended Data 2a). That VMHvl^{ERα} neurons respond highly to estrogen, but not to fasting[11], suggests that fluctuating hormones rather than hunger engage these neurons, setting the stage for behavioral changes across the reproductive cycle.

MC4R Levels Controlled by Estrogen

Candidate mediators of ERα signaling were identified after profiling the VMHvl transcriptome in OVX mice treated with vehicle or EB (Fig. 1d). Among differentially expressed genes we noted enrichment of peptidergic G-protein coupled receptors, *Mc4r*, *Nmur2*, *Npy1r*, and *Ghsr*, and known estrogen-dependent genes (*Greb1*, *Pgr*[4]), some of which are linked to locomotor activity (MP:0003313, adjusted P= 3.19E-4), (Extended Data 2d,e). We focused on *Mc4r* given its expression in the VMH[12], its role in locomotor behavior[13,14], and observed sex differences in *Mc4r* loss-of-function mutations in mice[13,15] and humans[9,16]. *Mc4r* was induced in females during proestrus (P) but not in estrus (E)

nor in intact males (Fig. 1e). We confirmed increased *Mc4r* expression in VMHvl neurons during proestrus or after EB treatment that colocalized with ERα (*Esr1*) and *Rprm*, a VMHvl female-specific marker[7] (Fig. 1f and Extended Data 2f-i).

We further established that *Mc4r* is a direct transcriptional target of ERα using CUT&RUN (Cleavage Under Targets and Release Using Nuclease), a technique that detects transient in vivo binding events within heterogenous tissues[17]. As expected, hormone-dependent ERα-chromatin interactions were detected in *Greb1* and *Pgr* (Extended Data 3a,b). High sensitivity afforded by CUT&RUN enabled detection of two conserved ERα binding sites within the *Mc4r* locus (Fig. 1g, and Extended Data 3c,d). The first, located - 210kb downstream of the transcript, contains a canonical estrogen response element (ERE) consensus sequence. The second, in the proximal promoter, consists of an ERE half-site and a site for the trans-acting transcription factor 1 (Sp1) that together coordinate estrogen-dependent global regulation of ERα target genes[18]. An ERE was detected +200kb upstream of *Nmur2*, consistent with its upregulation during proestrus (Fig. 1g and Extended Data 2e, 3e). These data establish a direct molecular link between ERα and MC4R and imply that estrogen dynamically regulates the responsiveness of VMHvl^{ERα} neurons to neuropeptides.

VMHvl^{Mc4R} Neurons Project to Arousal Centers

ERα and MC4R coexpression, assessed using a Cre-dependent reporter crossed with *Mc4r-t2a-Cre* (Ai14^{Mc4r}), revealed that VMHvl$^{ERα/MC4R}$ neurons are a subset of the VMHvl^{ERα} population (Fig. 2a). This near-perfect concordance of Ai14^{Mc4r} and ERα and stage-dependent *Mc4r* induction was not detected in the medial amygdala (MeA) (Fig. 2a and Extended Data 4a,b). ERα was undetected in the paraventricular hypothalamus (PVH), a primary site that couples MC4R with food intake (Fig. 2a).

We then asked how afferent VMHvl^{MC4R} neuron projections, labeled by Cre-dependent, membrane-targeted YFP (mYFP), compared to the broader VMHvl^{ERα} population[19] (Fig. 2b). Overall, while many (~84%) of the same major projections reported for VMHvl^{ERα} neurons were identified, robust targeting to the ARC and medial amygdala (MeA) was not observed (Fig. 2c,d Cluster I and Extended Data 4c,d). Unexpectedly, VMHvl^{MC4R} neurons projected to the dorsal CA1 (CA1d) and the adjacent subiculum (SUBd) (Fig. 2c,d Cluster II), a hippocampal region controlling locomotor speed in mice[20] and containing “speed cells” whose firing rate correlates with velocity[21]. Expected projections from VMHvl^{MC4R} neurons to the midbrain pre-motor periaqueductal grey (PAG) region showed a unique pattern restricted to the lateral and dorsolateral PAG columns (PAGdl/l) associated with escape behaviors[22], while conspicuously avoiding the ventrolateral PAG (PAGvl), involved in freezing and defensive behaviors[23] (Extended Data 4e). VMHvl^{MC4R} neurons also projected to the hindbrain pontine region containing a cluster of nuclei that mediate sexual receptivity and locomotor arousal[24,25].

Activating VMHvl^{Mc4R} Node Offsets Estrogen Loss

To assess the functional output of VMHvl$^{ERα/MC4R}$ neurons we stimulated this population using Cre-dependent DREADDs (Designer Receptors Exclusively Activated by Designer

Drugs, AAV-DIO-hM3Dq-mCherry) injected bilaterally into the VMHvl of *Mc4r-t2a-Cre* and control littermates (Fig. 3a). Administration of clozapine-n-oxide (CNO) during the inactive period (Light) significantly increased spontaneous physical activity in female and male VMHvl$^{MC4R::hM3Dq}$ mice, but not in VMHvl^{Cre-} controls (Fig. 3b and Extended Data 5a). Responses to a single injection of CNO lasted approximately five hours in VMHvl$^{MC4R::hM3Dq}$ mice, with the distance traveled jumping by 700% concomitant with a precipitous drop in immobile behavior (Extended Data 5b).

Aside from increased movement, other metabolic functions were insensitive to VMHvl^{MC4R} neuron stimulation. For example, compared to β−3 adrenergic agonist, CL (CL-316–243), CNO failed to elevate iBAT temperature or *Ucp1* in VMHvl$^{MC4R::hM3Dq}$ mice (Fig. 3c and Extended Data 5c,d). Glucose homeostasis was unchanged in CNO-treated VMHvl$^{MC4R::hM3Dq}$ mice; albeit the higher body weights inherent to the *Mc4r-t2a-Cre* line increased fasting glucose (Extended Data 5e,f). Food intake was unaffected by stimulation during the light period and decreased modestly during the dark period (Fig. 3d and Extended Data 5g). Providing CNO in the drinking water over 24 hours led to a nearly 10% drop in body weight in VMHvl$^{MC4R::hM3Dq}$ females with a corresponding increase in activity (Fig. 3e, Supplementary Video, and Extended Data 5h-j) and resulted in a 13% drop in body weight when extended over eight days (Extended Data 5k). Conversely, targeting the VMHvl with inhibitory DREADDs (AAV-DIO-hM4Di-mCherry) increased sedentary behavior during the dark period following administration of the DREADD ligand, deschloroclozapine (DCZ) (Fig. 3f,g and Extended Data 5l,m). Thus, the marked changes in physical activity following chemogenetic or genetic manipulation of VMHvl$^{ERα/MC4R}$ cells imply that this neuron cluster is an essential generator for maximal physical activity in female mice and constitutes a potent node for promoting physical activity, which can be artificially engaged in both sexes.

Increased sedentary behavior and metabolic decline are hallmarks of declining estrogen during aging. We asked if DREADD-activation of VMHvl^{MC4R} neurons overrides these deleterious features in estrogen-depleted OVX female mice. Stimulating VMHvl^{MC4R} neurons over a short 24 hr period fully restored physical activity parameters and promoted significant weight loss in OVX females (Fig. 3h and Extended Data 6a,b). Stimulating this node in OVX females challenged with a high-fat diet (HFD) (Extended Data 6c) reversed the overt metabolic impairment due to estrogen depletion and chronic overnutrition. Fasting glucose and insulin tolerance improved notably after a single bout of CNO-induced activity in HFD-fed VMHvl$^{MC4R::hM3Dq}$ females (Extended Data 6d-f). Further, chronic stimulation of VMHvl^{MC4R} neurons in obese, sedentary OVX females resulted in a rapid, dramatic weight loss, accompanied by lowered fasting blood glucose, a drop in cellular adiposity of gonadal fat, and reduced plasma cholesterol (Fig. 3i,j and Extended Data 6g-i), all markers of improved metabolic health. Food intake was unaffected (Extended Data 6j). Hence, engagement of the VMHvl^{MC4R} activity node reduces body weight in OVX females and improves metabolic health in the face of a dietary challenge and estrogen depletion.

MC4R Gene Editing in VMHvl Drives Activity Long-Term

To determine whether melanocortin signaling itself regulates this VMHvl activity node, we initially confirmed that MT-II, a synthetic MC4R agonist, evoked cFOS expression in female mice pretreated with EB but not with vehicle (Extended data 7a,b). We next used the Cre-dependent *Mc4r*^{loxTB} allele[26] in combination with the *Sf1-Cre* transgene, which only overlaps with *Mc4r* expression in the VMH (Extended data 7c) to restore *Mc4r* in the VMH of otherwise null mice (*Mc4r*$^{Sf1\text{-}Cre}$). In response to EB, this rescue approach increased *Mc4r* expression in VMHvl^{Esr1} neurons, similar to wild type (*Mc4r*$^{+/+}$) females (Fig. 4a). Body weights were equivalent at weaning (Extended Data 7d). Consistent with loss of PVH MC4R signaling, null *Mc4r*^{loxTB} and rescued *Mc4r*$^{Sf1\text{-}Cre}$ females developed obesity, hyperphagia, and increased body-lengths[26] compared to control littermates. However, restoring *Mc4r* in the VMHvl attenuated overt weight gain and sedentary behavior in female but not male *Mc4r*$^{Sf1\text{-}Cre}$ mice (Fig. 4b,e and Extended Data 7d-g). Thus, our data solidify the role of MC4R signaling in the female VMHvl for promoting spontaneous activity.

To verify that MC4R signaling is an integral component of the hormone-responsive VMHvl activity node, CRISPR-mediated activation (CRISPRa) was employed to increase *Mc4r* expression. Previously, in haploinsufficient *Mc4r*$^{+/-}$ mice, gene dosage and energy imbalance were normalized by CRISPRa targeting the PVH[27]. Here, wild type female and male mice were stereotaxically injected with a dual vector system containing guide RNA targeting the *Mc4r* promoter ERE half-site (AAV-*Mc4r*-Pr-sgRNA) and dCas9 tethered to the VP64 transcriptional activator (AAV-dCas9-VP64) to selectively upregulate *Mc4r* expression in the VMHvl (Fig. 4f). Control mice received dCas9-VP64 without sgRNA. Delivery of *Mc4r*-CRISPRa-viral vectors to the VMHvl was confirmed post-mortem and revealed moderate but long-lived induction of *Mc4r* in both sexes (Fig. 4g and Extended Data 8a-c). CRISPRa^{Mc4r} females traveled twice the distance in the dark compared to controls, with increased movement persisting for at least 17 weeks post-injection (Fig. 4h,i). Activity in CRISPRa^{Mc4r} males also increased, and in both sexes the drop in sedentary behavior in CRISPRa^{Mc4r} mice was restricted to nighttime, thus preserving regular diurnal activity patterns (Fig. 4i and Extended Data 8d,e). The lack of weight loss in female CRISPRa^{Mc4r} mice may reflect the modest but significant increase in daily food intake in females. BAT activity was unchanged (Extended Data 8f-h). Weeks of elevated physical activity (and mechanical loading) in CRISPRa^{Mc4r} females, increased cortical bone thickness and bone volume (Fig. 4j and Extended Data 8i). Under these conditions, CRISPRa^{Mc4r} failed to restore normal activity in OVX females (Extended Data 8j-l). Hence, sidestepping ERα and directly increasing *Mc4r* dosage in the VMHvl permanently increases spontaneous activity behavior in both sexes.

Concluding Remarks

Here, we identify an estrogen sensitive VMHvl$^{ERα/MC4R}$ node that maximizes daily patterns of spontaneous physical activity in female mice. MC4R is an essential intermediary component coupling estrogen and energy expenditure as a direct ERα transcriptional target (Fig. 4k). Thus, as *Mc4r* expression increases during the pre-ovulatory period, sensitivity to melanocortin rises in the VMHvl, resulting in spikes of estrogen-dependent activity first

described in 1924[ref28], thus illuminating how estrogen drives behavioral outputs during a critical point in the reproductive cycle.

As human gain-of-function *MC4R* variants reduce receptor turnover and protect against weight gain[29], identifying endogenous signals that modulate MC4R expression becomes of interest. We identify estrogen as a potent inducer of *Mc4r* expression. The high degree of conservation in consensus ERE binding motifs in the mammalian *Mc4r* locus suggests that estrogen similarly upregulates human *MC4R* expression. MC4R agonists that elicit sexual behaviors in estrogen-primed female rodents[30] and enhance libido in premenopausal women suffering from hypoactive sexual desire disorder[31] may act by directly targeting the VMHvl$^{ERα/MC4R}$ node. Once engaged, VMHvl^{MC4R} neurons target CNS regions involved in reproductive behaviors, as well as sites in the hippocampal region that regulate speed and orientation of locomotion[20,21], and in hindbrain regions associated with arousal and motor output[32]. It remains to be determined if these VMHvl outputs contribute to psychiatric disorders (e.g., postpartum depression, premenstrual dysphoric disorder) that coincide with periods of hormonal fluctuations. Conversely, curtailment of *MC4R* expression following estrogen depletion might underlie the increased sedentary lifestyle associated with menopause[33].

Despite the pronounced rise in physical activity in CRISPRa^{Mc4r} females, body weights remained stubbornly constant in the face of small increases in daily food intake. Whereas DREADD activation of VMHvl^{MC4R} neurons reduced body weight rapidly in estrogen depleted OVX females, this rate of weight loss was not sustainable (Extended Data 7g). Collectively, these results reinforce the notion that engagement of adaptive responses limits exercise-induced weight loss[34]. Nonetheless, decreasing sedentary behavior reduces the risk of metabolic- and age-related co-morbidities, including heart disease, frailty, cancer, and infectious diseases[35]. As such, the extremely durable increase in spontaneous physical activity achieved by the non-transgenic CRISPRa^{Mc4r} approach provides a unique preclinical model to explore the motivational aspects and health benefits of an active lifestyle. Our findings underscore the benefits of estrogen in minimizing sedentary behavior and provoke further discussion about hormone replacement therapies in postmenopausal women.

Extended Data

Extended Data Table 1:

Brain Region Abbreviations

Abbreviation	Full Name
3V	Third Ventricle
4V	Fourth Ventricle
ac	Anterior Commissure
AHN	Anterior Hypothalamic Nucleus
AQ	Cerebral Aqueduct
ARC	Arcuate Nucleus

Abbreviation	Full Name
AVPV	Anteroventral Periventricular Nucleus
B	Barrington's Nucleus
BSTam	Bed Nuclei of the Stria Terminalis, anterior division, anteromedial area
BSTpr	Bed Nuclei of the Stria Terminalis, posterior division, principal nucleus
CA1d	Dosal Ammon's Horn, field CA1
CeA	Central Amygdalar Nucleus
CENT2	Central Lobule II
cpd	Cerebral Peduncle
d3V	Dorsal Third Ventricle
DG	Dentate Gyrus
DRN	Dorsal Raphe Nucleus
fr	Fasiculus Retroflexus
LC	Locus Coeruleus
LDTg	Laterodorsal Tegmental nucleus
LHb	Lateral Habenula
LSr	Lateral Septal Nucleus, rostral part
LV	Lateral Ventricle
ME	Median Eminence
MeA	Medial Amygdalar Nucleus
mlf	Medial Longitudinal Fascicle
MPO	Medial Preoptic Area
NPC	Nucleus of the Posterior Commissure
opt	Optic Tract
PAGdl/l	Periaqueductal Gray, dorsolateral/lateral
PAGdm	Periaqueductal Gray, dorsomedial
PAGvl	Periaqueductal Gray, ventrolateral
PBls	Parabrachial Nucleus, lateral division
pc	Posterior Commissure
PMv	Ventral Premammillary Nucleus
PN	Pontine Central Gray
PVH	Paraventricular Hypothalamic Nucleus
PVT	Paraventricular Nucleus of the Thalamus
SUBd	Dorsal Subiculum
ZI	Zona Incerta

Extended Data Table 2:

Statistical tests and results

Figure	Statistical Test	Result	Post Hoc Comparison(s)
1a, Body Weights	Unpaired 2-tailed *t* Test	$t_{(16)}$=2.365, P=0.0310	
1a, X-Ambulatory	2-Way ANOVA	interaction effect $F_{(1,15)}$=4.548, P=0.0499	Dark Period, VMHvl^{Control} vs VMHvl$^{ERα.KO}$ P=0.0014
1c, VMHvl	Unpaired 2-tailed *t* Test	$t_{(7)}$=6.074, P=0.0005	
1c, ARC	Unpaired 2-tailed *t* Test	$t_{(7)}$=1.562, P=0.1622	
1e, *Mc4r*	1-Way ANOVA	$F_{(2,14)}$=6.428, P=0.0105	E vs P P=0.0163, P vs ♂ P=0.0189, and E vs ♂ P=0.7764
2a, VMHvl	1-Way ANOVA	$F_{(2,24)}$=43.09, P<0.0001	ERα vs ERα/MC4R P<0.0001
2a, MeA	Unpaired 2-tailed t Test	F(2,9)=12.28, P=0.0027	MC4R vs ERα/MC4R P=0.0057
3b, Female Total Distance	RM 2-Way ANOVA	interaction effect $F_{(1,8)}$=27.48, P=0.0008	CNO, VMHvl^{Cre-} vs VMHvl$^{MC4R::hM3Dq}$ P<0.0001
3b, Male Total Distance	RM 2-Way ANOVA	interaction effect $F_{(1,7)}$=36.27, P=0.0005	CNO, VMHvl^{Cre-} vs VMHvl$^{MC4R::hM3Dq}$ P <0.0001
3c	RM 2-Way ANOVA	treatment effect $F_{(2,18)}$=18.50, P<0.0001	CL VMH^{Cre-} P<0.0001, CL VMHvl$^{MC4R::hM3Dq}$ P=0.0003
3e	RM 2-Way ANOVA	interaction effect $F_{(1,8)}$=45.30, P=0.0001	CNO, VMHvl^{Cre-} vs VMHvl$^{MC4R::hM3Dq}$ P <0.0001
3g, Distance % Change	Unpaired 2-tailed t Test	$t_{(10)}$=6.555, P<0.0001	
3g, Rearing % Change	Unpaired 2-tailed t Test	$t_{(10)}$=3.398, P=0.0068	
3g, Immobile % Change	Unpaired 2-tailed t Test	$t_{(10)}$=2.727, P=0.0213	
3h	1-Way ANOVA	$F_{(2,30)}$=27.88, P<0.0001	intact vs OVX P<0.0001, intact vs OVX+CNO P=0.0023, and OVX vs OVX+CNO P<0.0001
3i	RM 2-Way ANOVA	interaction effect $F_{(8,64)}$=24.40, P<0.0001	
3j	Nested *t* Test	$t_{(8)}$=3.447, P=0.0087	
4b, female 8 Weeks	1-Way ANOVA	$F_{(2,41)}$=188.5, P<0.0001	*Mc4r*$^{+/+}$ vs *Mc4r*^{loxTB} P<0.0001, *Mc4r*$^{+/+}$ vs *Mc4r*$^{Sf1\text{-}Cre}$ P<0.0001 and *Mc4r*$^{Sf1\text{-}Cre}$ vs *Mc4r*^{loxTB} P=0.0026
4b, male 8 weeks	1-Way ANOVA	$F_{(2,25)}$=92.31, P<0.0001	*Mc4r*$^{+/+}$ vs *Mc4r*^{loxTB} P<0.0001, *Mc4r*$^{+/+}$ vs *Mc4r*$^{Sf1\text{-}Cre}$ P<0.0001 and *Mc4r*$^{Sf1\text{-}Cre}$ vs *Mc4r*^{loxTB} P=0.1449
4c	1-Way ANOVA	$F_{(2,36)}$=25.25, P<0.0001	*Mc4r*$^{+/+}$ vs *Mc4r*^{loxTB} P<0.0001, *Mc4r*$^{+/+}$ vs *Mc4r*$^{Sf1\text{-}Cre}$ P<0.0001 and *Mc4r*$^{Sf1\text{-}Cre}$ vs *Mc4r*^{loxTB} P=0.9851
4d	1-Way ANOVA	$F_{(2,26)}$=5.465, P=0.0104	*Mc4r*$^{+/+}$ vs *Mc4r*^{loxTB} P=0.0196, *Mc4r*$^{+/+}$ vs *Mc4r*$^{Sf1\text{-}Cre}$ P=0.0171 and *Mc4r*$^{Sf1\text{-}Cre}$ vs *Mc4r*^{loxTB} P=0.4904
4e	RM 2-Way ANOVA	interaction effect $F_{(2,30)}$=6.4, P=0.0047	*Mc4r*$^{+/+}$ vs *Mc4r*^{loxTB} P<0.0001, *Mc4r*$^{+/+}$ vs *Mc4r*$^{Sf1\text{-}Cre}$ P=0.0503 and *Mc4r*$^{Sf1\text{-}Cre}$ vs *Mc4r*^{loxTB} P=0.0153

Figure	Statistical Test	Result	Post Hoc Comparison(s)
4i, female	RM 2-Way ANOVA	interaction effect $F_{(1,30)}$=32.82, P<0.0001	Dark Period, Control vs CRISPRa^{Mc4r} P <0.0001
4i, male	RM 2-way ANOVA	interaction effect $F_{(1,19)}$ =16.51, P=0.0007	Dark Period, Control vs CRISPRa^{Mc4r} P <0.0001
4j	Unpaired 2-tailed t Test	$t_{(6)}$=3.498, P =0.0129	

Supplementary Material

Refer to Web version on PubMed Central for supplementary material.

REFERENCES

1. Mauvais-Jarvis F, Clegg DJ & Hevener AL The role of estrogens in control of energy balance and glucose homeostasis. Endocr Rev 34, 309–338 (2013). [PubMed: 23460719]
2. Carr MC The emergence of the metabolic syndrome with menopause. J Clin Endocrinol Metab 88, 2404–2411 (2003). [PubMed: 12788835]
3. Correa SM, et al. An estrogen-responsive module in the ventromedial hypothalamus selectively drives sex-specific activity in females. Cell Rep 10, 62–74 (2015). [PubMed: 25543145]
4. Herber CB, et al. Estrogen signaling in arcuate Kiss1 neurons suppresses a sex-dependent female circuit promoting dense strong bones. Nat Commun 10, 163 (2019). [PubMed: 30635563]
5. Martinez de Morentin PB, et al. Estradiol regulates brown adipose tissue thermogenesis via hypothalamic AMPK. Cell Metab 20, 41–53 (2014). [PubMed: 24856932]
6. Xu Y, et al. Distinct hypothalamic neurons mediate estrogenic effects on energy homeostasis and reproduction. Cell Metab 14, 453–465 (2011). [PubMed: 21982706]
7. van Veen JE, et al. Hypothalamic estrogen receptor alpha establishes a sexually dimorphic regulatory node of energy expenditure. Nat Metab 2, 351–363 (2020). [PubMed: 32377634]
8. Farooqi IS, et al. Dominant and recessive inheritance of morbid obesity associated with melanocortin 4 receptor deficiency. J Clin Invest 106, 271–279 (2000). [PubMed: 10903343]
9. Qi L, Kraft P, Hunter DJ & Hu FB The common obesity variant near MC4R gene is associated with higher intakes of total energy and dietary fat, weight change and diabetes risk in women. Hum Mol Genet 17, 3502–3508 (2008). [PubMed: 18697794]
10. Thammacharoen S, Lutz TA, Geary N & Asarian L Hindbrain administration of estradiol inhibits feeding and activates estrogen receptor-alpha-expressing cells in the nucleus tractus solitarius of ovariectomized rats. Endocrinology 149, 1609–1617 (2008). [PubMed: 18096668]
11. Villanueva EC, et al. Complex regulation of mammalian target of rapamycin complex 1 in the basomedial hypothalamus by leptin and nutritional status. Endocrinology 150, 4541–4551 (2009). [PubMed: 19628573]
12. Mountjoy KG, Mortrud MT, Low MJ, Simerly RB & Cone RD Localization of the melanocortin-4 receptor (MC4-R) in neuroendocrine and autonomic control circuits in the brain. Mol Endocrinol 8, 1298–1308 (1994). [PubMed: 7854347]
13. Ste Marie L, Miura GI, Marsh DJ, Yagaloff K & Palmiter RD A metabolic defect promotes obesity in mice lacking melanocortin-4 receptors. Proc Natl Acad Sci U S A 97, 12339–12344 (2000). [PubMed: 11027312]
14. Chen AS, et al. Role of the melanocortin-4 receptor in metabolic rate and food intake in mice. Transgenic Res 9, 145–154 (2000). [PubMed: 10951699]
15. Huszar D, et al. Targeted disruption of the melanocortin-4 receptor results in obesity in mice. Cell 88, 131–141 (1997). [PubMed: 9019399]

16. Sina M, et al. Phenotypes in three pedigrees with autosomal dominant obesity caused by haploinsufficiency mutations in the melanocortin-4 receptor gene. Am J Hum Genet 65, 1501–1507 (1999). [PubMed: 10577903]
17. Skene PJ, Henikoff JG & Henikoff S Targeted in situ genome-wide profiling with high efficiency for low cell numbers. Nat Protoc 13, 1006–1019 (2018). [PubMed: 29651053]
18. Lin CY, et al. Whole-genome cartography of estrogen receptor alpha binding sites. PLoS Genet 3, e87 (2007). [PubMed: 17542648]
19. Lo L, et al. Connectional architecture of a mouse hypothalamic circuit node controlling social behavior. Proc Natl Acad Sci U S A 116, 7503–7512 (2019). [PubMed: 30898882]
20. Fuhrmann F, et al. Locomotion, Theta Oscillations, and the Speed-Correlated Firing of Hippocampal Neurons Are Controlled by a Medial Septal Glutamatergic Circuit. Neuron 86, 1253–1264 (2015). [PubMed: 25982367]
21. Gois Z & Tort ABL Characterizing Speed Cells in the Rat Hippocampus. Cell Rep 25, 1872–1884 e1874 (2018). [PubMed: 30428354]
22. Evans DA, et al. A synaptic threshold mechanism for computing escape decisions. Nature 558, 590–594 (2018). [PubMed: 29925954]
23. Tovote P, et al. Midbrain circuits for defensive behaviour. Nature 534, 206–212 (2016). [PubMed: 27279213]
24. Carter ME, et al. Tuning arousal with optogenetic modulation of locus coeruleus neurons. Nat Neurosci 13, 1526–1533 (2010). [PubMed: 21037585]
25. Coimbra B, et al. Role of laterodorsal tegmentum projections to nucleus accumbens in reward-related behaviors. Nat Commun 10, 4138 (2019). [PubMed: 31515512]
26. Balthasar N, et al. Divergence of melanocortin pathways in the control of food intake and energy expenditure. Cell 123, 493–505 (2005). [PubMed: 16269339]
27. Matharu N, et al. CRISPR-mediated activation of a promoter or enhancer rescues obesity caused by haploinsufficiency. Science 363(2019).
28. Slonaker JR The Effect of Pubescence, Oestruatlon and Menopause on the Voluntary Activity in the Albino Rat. Am. J. Physiol 68, 294–315 (1924).
29. Lotta LA, et al. Human Gain-of-Function MC4R Variants Show Signaling Bias and Protect against Obesity. Cell 177, 597–607 e599 (2019). [PubMed: 31002796]
30. Pfaus JG, Shadiack A, Van Soest T, Tse M & Molinoff P Selective facilitation of sexual solicitation in the female rat by a melanocortin receptor agonist. Proc Natl Acad Sci U S A 101, 10201–10204 (2004). [PubMed: 15226502]
31. Clayton AH, et al. Bremelanotide for female sexual dysfunctions in premenopausal women: a randomized, placebo-controlled dose-finding trial. Womens Health (Lond) 12, 325–337 (2016). [PubMed: 27181790]
32. Chandler DJ, et al. Redefining Noradrenergic Neuromodulation of Behavior: Impacts of a Modular Locus Coeruleus Architecture. J Neurosci 39, 8239–8249 (2019). [PubMed: 31619493]
33. Duval K, et al. Effects of the menopausal transition on energy expenditure: a MONET Group Study. Eur J Clin Nutr 67, 407–411 (2013). [PubMed: 23422924]
34. O'Neal TJ, Friend DM, Guo J, Hall KD & Kravitz AV Increases in Physical Activity Result in Diminishing Increments in Daily Energy Expenditure in Mice. Curr Biol 27, 423–430 (2017). [PubMed: 28111149]
35. Duggal NA, Niemiro G, Harridge SDR, Simpson RJ & Lord JM Can physical activity ameliorate immunosenescence and thereby reduce age-related multi-morbidity? Nat Rev Immunol 19, 563–572 (2019). [PubMed: 31175337]

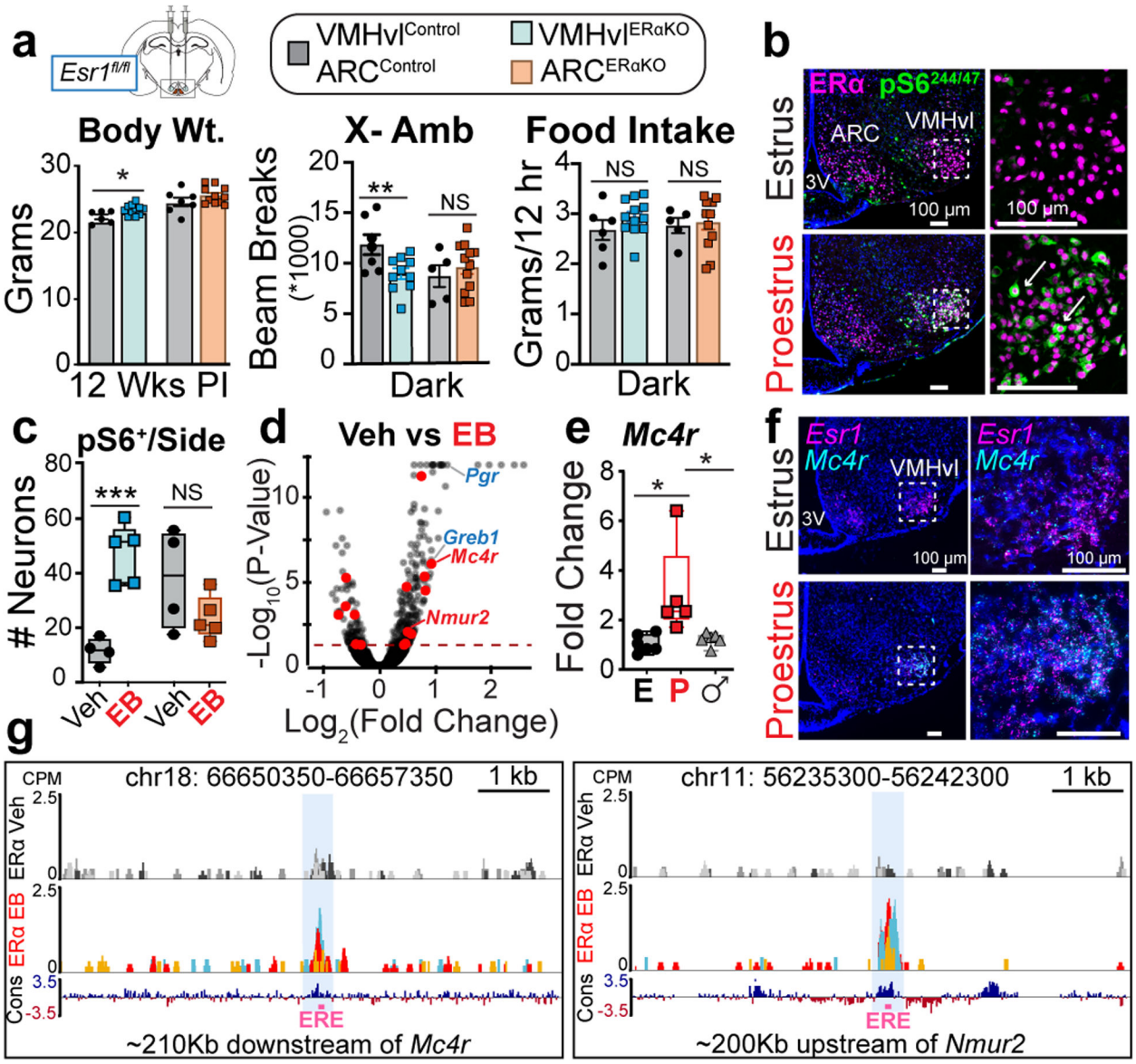

Fig. 1. VMHvl neurons are sensitive to estrogen and maintain energy expenditure in adult females.

a, Body weight (**P*=0.0310), ambulatory activity (***P*=0.0014), and food intake in VMHvl^{ERαKO} (n=10), ARC^{ERαKO} (n=12), and control (grey, n=7/5) females. **b,** ERa and pS6$^{244/47}$ co-expression (arrows) in proestrus and estrus (representative of 5 mice). **c,** Number of pS6$^{244/47}$-labeled VMHvl (****P*=0.0005) and ARC cells in vehicle (n=4) or EB (n=5) treated females. **d**, Enrichment of peptide ligand-binding receptors (red) (Benjamini-Hochburg adjusted *P*<0.05, dashed line). **e,** VMHvl *Mc4r* expression in proestrus (n=5), male (♂, n=6, **P*=0.0189) and estrus (n=5, **P*=0.0163) mice. **f,** *Mc4r* and *Esr1* expression in estrus and proestrus (representative of 5 mice). **g,** CPM-normalized coverage tracks of ERE-containing ERα binding sites (pink boxes) within *Mc4r* (2/3 biological replicates) and *Nmur2* (2/3 biological replicates) loci (MACS2, q < 0.01) in sub-cortical nuclei from vehicle and EB treated gonadectomized mice. Data are mean ± SEM, scatter, or box plots (whiskers

indicate minimum and maximum values, edges of box are 25th and 75th percentiles, and center line indicates mean). **a, c,** unpaired 2-tailed *t* Test; **a,** RM 2-way ANOVA; **e,** 1-way ANOVA. Holm-Šidák multiple comparisons.

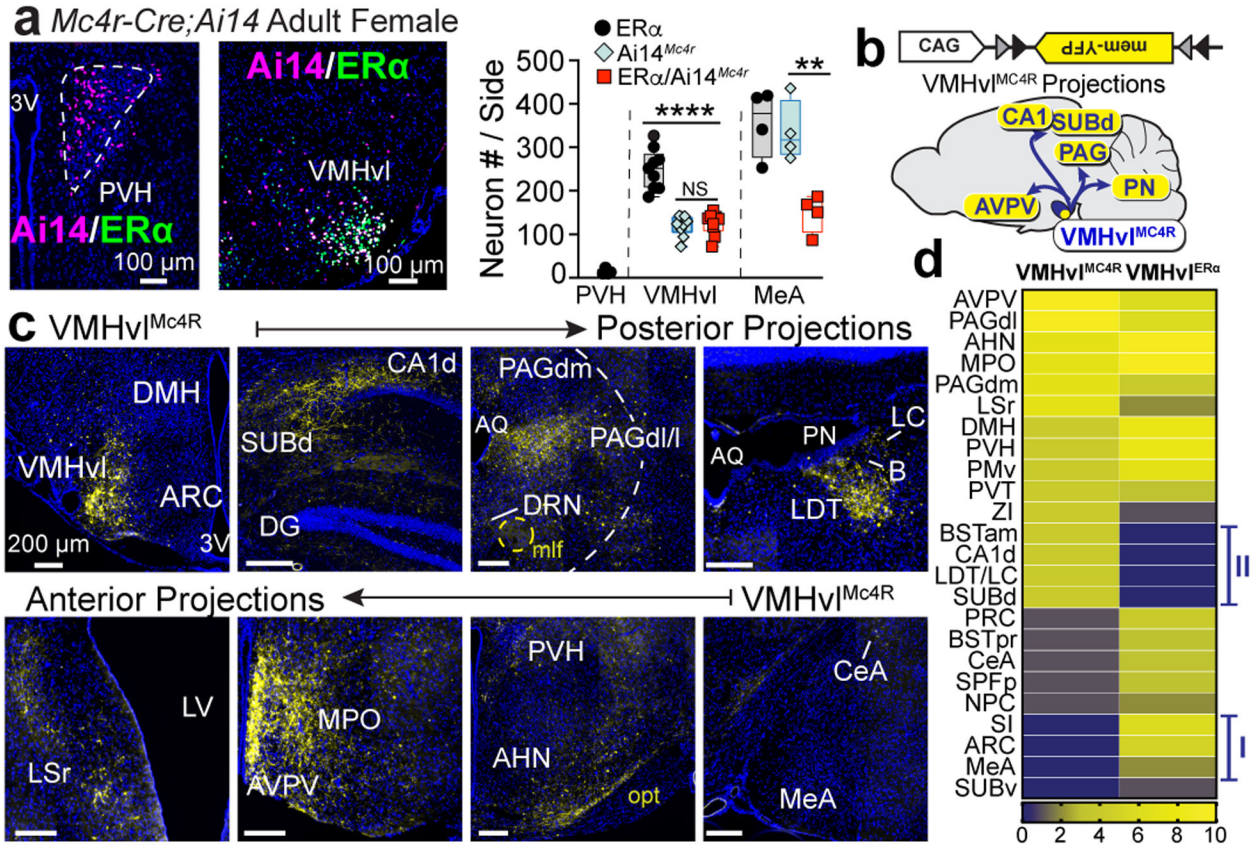

Figure 2. VMHvl^{MC4R} neurons are molecularly and anatomically distinct subset of VMHvl^{ERα} neurons.

a, ERα and Ai14 expression and quantification in the PVH (n=4), VMHvl (n=9, **** P<0.0001), and MeA (n=4, ** P=0.0057) of Ai14^{Mc4r} female mice. **b**, Labeling vector and map of major VMHvl^{MC4R} projections. **c,** VMHvl projections to anterior (upper row) and posterior (lower row) regions. Images representative of bilateral VMHvl targeting (n=3 mice, scale bars=200µm). **d**, Semi-quantitative comparison of VMHvl^{MC4R} and VMHvl^{ERα} projection[19] intensities. Anatomical abbreviations in Extended Data Table 1. See Fig. 1c legend for box plot description. **a,** 1-way ANOVA Holm-Šidák multiple comparisons.

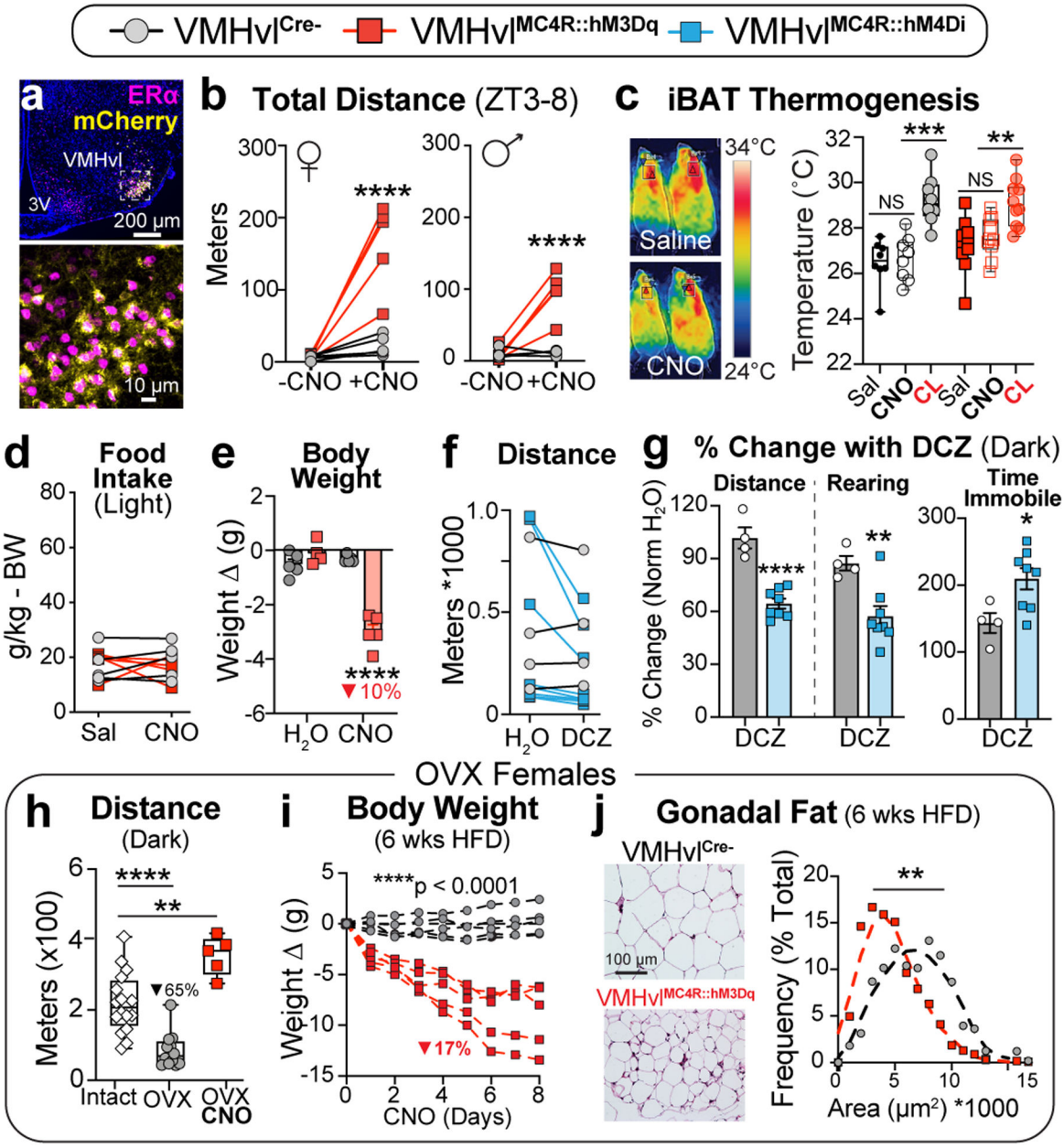

Fig. 3. VMHvl^{MC4R} neurons control physical activity levels and when stimulated reverse inactivity and hypometabolism in obese OVX females.

a, ERα and mCherry in VMHvl$^{MC4R::hM3Dq}$ female. **b,** Spontaneous activity in VMHvl$^{MC4R::hM3Dq}$ (female=5, ****P<0.0001, male=5, ****P<0.0001) and VMHvl^{Cre-} (female=5, male=4) mice ± CNO injection. **c**, Thermography of VMHvl^{Cre-} (left) and VMHvl$^{MC4R::hM3Dq}$ (right) females and iBAT surface temperatures 30 and 45 min after Sal, CNO, or CL injection (n=4/5 VMHvl^{Cre-} P<0.0001, VMHvl$^{MC4R::hM3Dq}$ P=0.0003). **d,** Body weight normalized food consumption in females (n=5/5) following Sal/CNO injection during light period (ZT4–9). **e**, 24-hour weight change in females (n=5/5) administered drinking water (H2O) or CNO-water (CNO, ****P<0.0001). **f**, **g,** Dark period (ZT12–24) activity in VMHvl$^{MC4R::hM4Di}$ (n=8) and VMHvl^{Cre-} (n=4) females administered water or

DCZ-water. ****P<0.0001, **P=0.0068, *P=0.0213. **h,** Activity levels in intact (n=16), OVX (n=12, ****P<0.0001), and OVX+CNO VMHvl$^{MC4R::hM3Dq}$ (n=5, **P=0.0023) mice. **i, j,** Body weight and gonadal white adipocyte area following 8-day CNO treatment of OVX/HFD mice (n=5/5). Data are mean ± SEM, scatter, or box plots (see Fig. 1c legend). **b, c, d, e, f, h,** RM 2-way ANOVA; **g,** unpaired 2-tailed t Tests; **h,** 1-way ANOVA; **i,** nested t Test. Holm-Šidák multiple comparisons as appropriate.

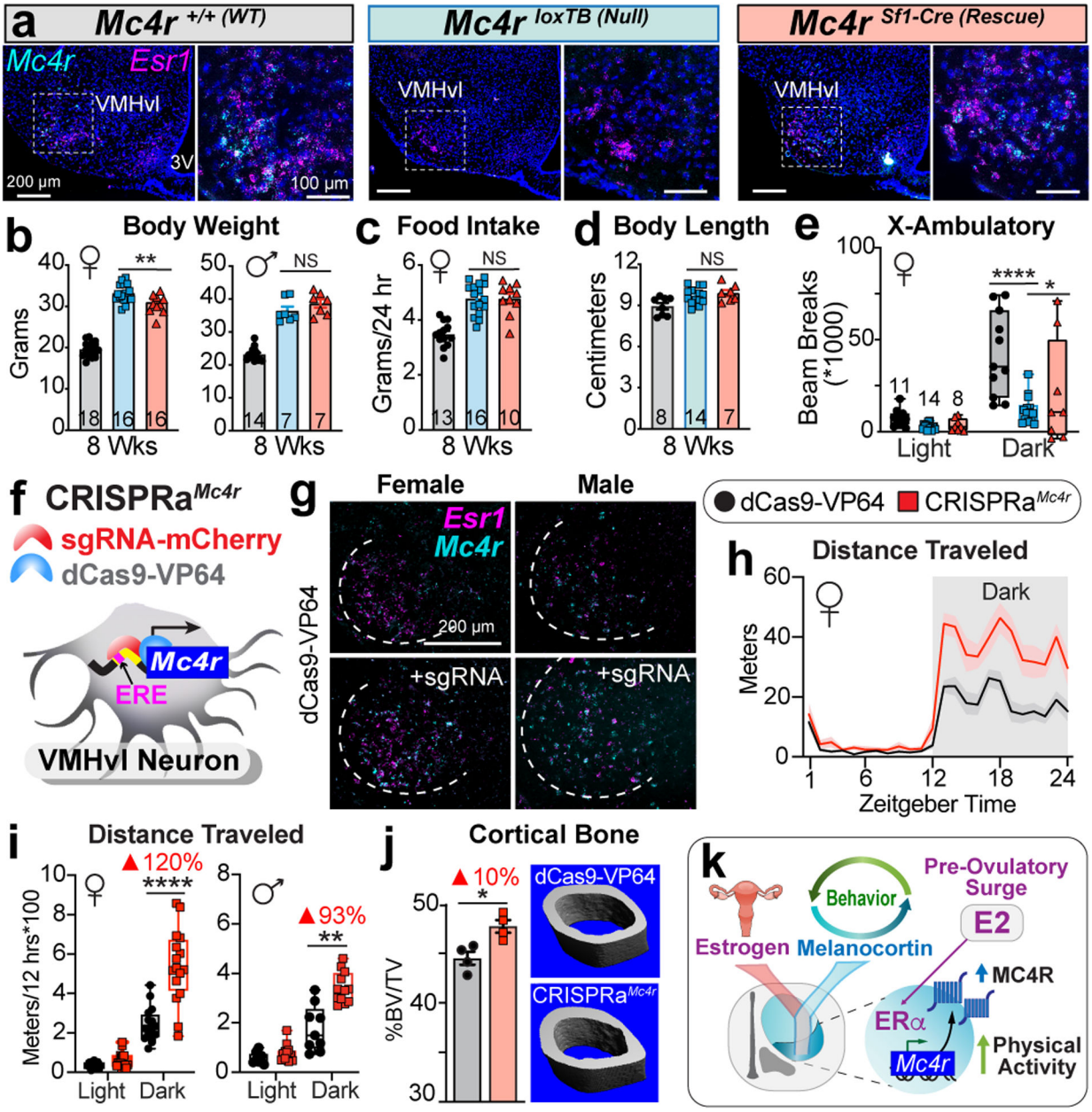

Fig. 4. Sex-specific role for MC4R signaling in the VMHvl can be bypassed using CRISPR-mediated activation.

a, *Esr1* and *Mc4r* expression in $Mc4r^{+/+}$, $Mc4r^{loxTB,}$ and $Mc4r^{Sf1\text{-}Cre}$ females. **b**, Body weights in 8-week-old female (**P=0.0026) and male $Mc4r^{+/+}$, $Mc4r^{loxTB}$, and $Mc4r^{Sf1\text{-}Cre}$ mice. **c**, Food intake in female cohorts. **d,** Body length in female cohorts. **e**, Light and dark period activity in females (****P<0.0001, *P=0.0153). **e**, $CRISPRa^{Mc4r}$ targets *Mc4r* promotor. **f,** *Esr1* and *Mc4r* expression in control and $CRISPRa^{MC4R}$ female and male mice. **g**, Home-cage activity in $CRISPRa^{Mc4r}$ (n=6) and control (n=5) female mice. **h,** Distances for three most active runs from $CRISPRa^{Mc4r}$ and control female (n=6/5, ****P<0.0001) and male (n=4/3) mice. **i**, Cortical bone volume fraction for female mice 4 months post-infection (P=0.0129). **j,** $VMHvl^{ERα/MC4R}$ neurons integrates estrogen and melanocortin

signaling to generate a specialized hormone-dependent activity node in females. Data are mean ± SEM or box plots (see Fig. 1c legend). **b, c,** 1-way ANOVA; **d, h,** RM 2-way ANOVA; Holm-Šidák multiple comparisons. **i,** unpaired 2-tailed t Tests.